

# Universality, Robustness, and Limits of the Eigenstate Thermalization Hypothesis in Open Quantum Systems

Gabriel Almeida,<sup>1,\*</sup> Pedro Ribeiro,<sup>1,2,†</sup> Masudul Haque,<sup>3</sup> and Lucas Sá<sup>4,‡</sup>

<sup>1</sup>*CeFEMA-LaPMET, Departamento de Física, Instituto Superior Técnico, Universidade de Lisboa, Av. Rovisco Pais, 1049-001 Lisboa, Portugal*

<sup>2</sup>*Beijing Computational Science Research Center, Beijing 100193, China*

<sup>3</sup>*Institut für Theoretische Physik, Technische Universität Dresden, 01062 Dresden, Germany*

<sup>4</sup>*TCM Group, Cavendish Laboratory, University of Cambridge, JJ Thomson Avenue, Cambridge CB3 0HE, UK*

The eigenstate thermalization hypothesis (ETH) underpins much of our modern understanding of the thermalization of closed quantum many-body systems. Here, we investigate the statistical properties of observables in the eigenbasis of the Lindbladian operator of a Markovian open quantum system. We demonstrate the validity of a *Lindbladian ETH ansatz* through extensive numerical simulations of several physical models. To highlight the robustness of Lindbladian ETH, we consider what we dub the dilute-click regime of the model, in which one postselects only quantum trajectories with a finite fraction of quantum jumps. The average dynamics are generated by a non-trace-preserving Liouvillian, and we show that the Lindbladian ETH ansatz still holds in this case. On the other hand, the no-click limit is a singular point at which the Lindbladian reduces to a doubled non-Hermitian Hamiltonian and Lindbladian ETH breaks down.

*Introduction.*—Great insight has been gained by treating the complex interactions of chaotic closed many-body quantum systems as if they were random because, in many ways, the Hamiltonian of these systems behaves as a large random matrix. For example, using random matrix theory (RMT), we can predict the structure of the matrix elements of an observable  $O$  in the energy eigenbasis  $|n\rangle$ , defined by  $H|n\rangle = E_n|n\rangle$ . They are given by

$$\langle m|O|n\rangle = \bar{O}\delta_{mn} + S_{mn}\sqrt{\frac{\overline{O^2}}{\mathcal{D}}}, \quad (1)$$

where  $\bar{O}$  (resp.  $\overline{O^2}$ ) is the average value of  $O$  (resp.  $O^2$ ),  $S_{mn}$  is a random variable with zero mean and unit variance and  $\mathcal{D}$  is the dimension of the Hilbert space.

The eigenstate thermalization hypothesis (ETH) [1, 2] states that the matrix elements of a local observable in a physical system also have the structure of Eq. (1), provided that  $\bar{O}$  and  $\overline{O^2}$  are replaced by smooth functions of the energy, which are identified with the microcanonical averaged value of  $O$  and  $O^2$ , respectively. It ensures that fluctuations around the microcanonical value of the observable are suppressed in the thermodynamic limit, thus matching the temporal average of  $O$  with the value expected from statistical mechanics. ETH is thus central to understanding thermalization, as it provides a mechanism by which isolated quantum systems can thermalize and there is extensive numerical evidence supporting it [3–10]. In contrast, violations of ETH can occur in specific contexts, such as integrable and many-body localized systems [7, 11–19], where an extensive number of conservation laws prevent thermalization, and systems exhibiting quantum many-body scars [20–24], in which a subset of quantum states avoid ergodicity.

Given the profound consequences of ETH on the dynamics of closed quantum systems, it is natural to ask if

there is an analogous result for open quantum systems, which interact with their environment and give rise to mixed states. In recent years, some progress has been made in this direction [25–30]. In some limits, open quantum systems can be modeled by non-Hermitian Hamiltonians [31]. While not conserving probability, such a description can be appropriate for short-time evolutions or when postselecting jump-free quantum trajectories. ETH still holds for these systems [28], provided that one computes the matrix elements with the basis of right (or left) eigenvectors,  $|r_n\rangle$  (or  $|l_n\rangle$ ), and one introduces a term that accounts for the nonorthogonality of the eigenvectors. The non-Hermitian ETH ansatz is then [28]

$$\langle r_m|O|r_n\rangle = \bar{O}\langle r_m|r_n\rangle + S_{mn}\sqrt{\frac{\overline{O^2}}{\mathcal{D}}}. \quad (2)$$

If the Hamiltonian is Hermitian, we have  $\langle r_m|r_n\rangle = \delta_{mn}$  and recover Eq. (1). This choice of matrix elements is crucial since it was proven [27] that there is no ETH for biorthogonal matrix elements such as  $\langle l_m|O|r_n\rangle$ .

A more complete description of open quantum systems employs a quantum master equation for the system's reduced density matrix  $\rho$ ,  $\dot{\rho} = \mathcal{L}[\rho]$ , where  $\mathcal{L}$  is the Liouvillian superoperator [32]. If the environment is Markovian, the Liouvillian takes the Lindblad form [33, 34]:

$$\mathcal{L}[\rho] = -i[H, \rho] + \sum_{k=1}^r \left( W_k \rho W_k^\dagger - \frac{1}{2} \{W_k^\dagger W_k, \rho\} \right). \quad (3)$$

Here,  $H$  is the Hamiltonian of the system and  $W_k$  (with  $k = 1, \dots, r$ ) are the jump operators describing the coupling to the environment.

Whereas in equilibrium the eigenstates of the Hamiltonian and the (thermal) steady state coincide, nonequilibrium dynamics offer the more intriguing possibility of

independently probing the structure of the eigenstates of the dynamical generator and steady state. The latter allows a straightforward extension [25] of ETH, even far from equilibrium [29], by writing it as the exponential of an effective Hamiltonian, to which Eq. (1) applies. In this Letter, we instead focus on the former, with our main results summarized as follows. Inspection of the time evolution of observables suggests that the role of matrix elements in the Hamiltonian eigenbasis is played in this context by overlaps of observables with (operator) eigenstates of the Lindbladian superoperator. Treating these eigenstates as random vectors leads to a *Lindbladian ETH ansatz*, whose validity and universality we test in three increasingly realistic physical models. Moreover, we conjecture that the ansatz is robust to any deformations that preserve the two-copy structure of the Lindbladian and show this explicitly for non-trace-preserving dynamics. Such dynamics can be obtained by averaging over quantum trajectories postselected to have a fixed rate of quantum jumps—what we dub the *dilute-click limit* and which continuously interpolates between Lindbladian dynamics and the no-click limit. In the latter, the Liouvillian decouples into two non-Hermitian Hamiltonians, and we show that Lindbladian ETH breaks down. In this limit, the eigenstates have additional structure, which adds a correction to the ansatz [28].

*Lindbladian ETH ansatz.*—In the Lindbladian setting, the time evolution of an observable  $O$  is given by

$$\langle O \rangle_t = \text{Tr}[O e^{\mathcal{L}t}[\rho]] = \sum_{\mu} e^{\lambda_{\mu}t} \text{Tr}[OR_{\mu}] \text{Tr}[L_{\mu}^{\dagger}\rho], \quad (4)$$

where  $\lambda_{\mu}$  are the eigenvalues of  $\mathcal{L}$ , while  $R_{\mu}$  and  $L_{\mu}$  are the respective right and left eigenoperators:  $\mathcal{L}[R_{\mu}] = \lambda_{\mu}R_{\mu}$  and  $\mathcal{L}^{\dagger}[L_{\mu}] = \lambda_{\mu}^*L_{\mu}$ . Additionally, we choose the normalization  $\text{Tr}[L_{\mu}^{\dagger}R_{\nu}] = \delta_{\mu\nu}$  and  $\|R_{\mu}\|^2 = \text{Tr}[R_{\mu}^{\dagger}R_{\mu}] = 1$ . To separate the scaling of  $O$  and  $\rho$  and to work with unit vectors, we can rewrite Eq. (4) as

$$\frac{\langle O \rangle_t}{\|O\| \cdot \|\rho\|} = \sum_{\mu} e^{\lambda_{\mu}t} \frac{\text{Tr}[OR_{\mu}]}{\|O\|} \frac{\text{Tr}[L_{\mu}^{\dagger}\rho]}{\|L_{\mu}\| \cdot \|\rho\|} \|L_{\mu}\|. \quad (5)$$

Therefore, we identify three important quantities for the dynamics:  $\text{OR}_{\mu} = \frac{\text{Tr}[OR_{\mu}]}{\|O\|}$ ,  $L\rho_{\mu} = \frac{\text{Tr}[L_{\mu}^{\dagger}\rho]}{\|L_{\mu}\| \cdot \|\rho\|}$  and  $\text{LL}_{\mu} = \|L_{\mu}\|^2 = \text{Tr}[L_{\mu}^{\dagger}L_{\mu}]$ . Related quantities have been studied in Ref. [26] that considered a disordered Ising chain with dissipation. For small disorder, the authors found that OR and  $L\rho$  are random variables with a complex Gaussian distribution, while LL is a random variable with a  $1/\gamma_2$  distribution. In this work, we show that these distributions hold for generic Markovian open quantum systems and, based on them, propose a Lindbladian ETH ansatz. For a generic chaotic Lindbladian, we thus have the following ansatz for the overlaps appearing in Eq. (5)

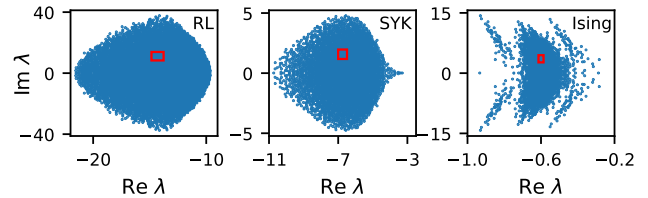


Figure 1. Spectrum of a random Liouvillian (left), the dissipative SYK model (center), and the damped Ising model (right). We study the local scalings and distributions of OR,  $L\rho$ , and LL in a small region of the spectrum (red box) defined by  $[\mu_x - \sigma_x/5, \mu_x + \sigma_x/5] \times [2\sigma_y/5, 4\sigma_y/5]$ , where  $\mu_x$  is the average value of  $\text{Re } \lambda$  and  $\sigma_x$  ( $\sigma_y$ ) is the standard deviation of  $\text{Re } \lambda$  ( $\text{Im } \lambda$ ).

(see also Ref. [26]):

$$\text{OR}_{\mu} = s_{\mu} \frac{f_1(\lambda_{\mu})}{\mathcal{D}}, \quad (6)$$

$$L\rho_{\mu} = s'_{\mu} \frac{f_2(\lambda_{\mu})}{\mathcal{D}}, \quad (7)$$

$$\text{LL}_{\mu} = r_{\mu} \mathcal{D}^2 f_3(\lambda_{\mu}). \quad (8)$$

Here,  $\mathcal{D}$  is the many-body Hilbert space dimension,  $s_{\mu}$  and  $s'_{\mu}$  are random variables with a complex normal distribution with mean zero and unit variance,  $r_{\mu}$  is a random variable with mean zero and unit variance, and  $f_i(\lambda_{\mu})$  are smooth functions of the Liouvillian eigenvalues [26]. This ansatz is justified by treating the  $\mathcal{D}^2$ -dimensional eigenvectors of  $\mathcal{L}$  as complex Gaussian random vectors. For example, for the OR overlap we have:

$$\overline{\text{Tr}[OR_n]} = \sum_i O_i^* \overline{R_{n,i}} = 0, \quad (9)$$

$$\begin{aligned} \overline{|\text{Tr}[OR_n]|^2} &= \sum_{i,j} O_i^* O_j \overline{R_{n,i} R_{n,j}^*} \\ &= \sum_{ij} O_i^* O_j \frac{\delta_{ij}}{\mathcal{D}^2} = \frac{\|O\|^2}{\mathcal{D}^2}. \end{aligned} \quad (10)$$

With the normalization  $\|R_{\mu}\|^2 = 1$ ,  $\text{LL}_{\mu}$  is the diagonal Chalker-Mehlig overlap of eigenvectors [35, 36], whose inverse was proven in Ref. [37] to follow a  $\gamma_2$  distribution. Below, we will verify the applicability of Eqs. (6)–(8) by computing the local scalings and distributions of OR,  $L\rho$ , and LL in different physical models.

*Physical models.*—To test the universality of the Lindbladian ETH ansatz, we study three disordered physical models with different degrees of locality, namely, a random-matrix Liouvillian [38–42], the dissipative Sachdev-Ye-Kitaev (SYK) model [43–47], and a damped disordered Ising chain [26]. The Liouvillian spectra of the three models are shown in Fig. 1.

We begin with the completely disordered case of random Liouvillians [41]. To obtain a random Liouvillian,

we draw a  $\mathcal{D} \times \mathcal{D}$  random Hermitian matrix  $H$  in Eq. (3) from the Gaussian unitary ensemble (GUE),

$$P_{\mathcal{D}}(H) \propto \exp \left\{ -\frac{1}{2} \text{Tr}[H^2] \right\}, \quad (11)$$

and  $r$  random non-Hermitian matrices  $W_k$  from the Ginibre unitary ensemble (GinUE),

$$P_{\mathcal{D}}(W_k) \propto \exp \left\{ -\frac{g^2}{2} \text{Tr}[W_k^\dagger W_k] \right\}, \quad (12)$$

from which we remove the trace,  $W_k \rightarrow W_k - \text{Tr}[W_k]$ . The variance  $g \equiv g_{\text{eff}}(4r\mathcal{D})^{-1/4}$  measures the dissipation strength [41]. In the following, we set  $r = 5$  and  $g_{\text{eff}} = 0.8$ .

Second, we consider the dissipative SYK model of  $N \in 2\mathbb{Z}$  Majorana fermions, which satisfy the Clifford algebra  $\{\chi_i, \chi_j\} = \delta_{ij}$ , with infinite-range two-body interactions in zero dimensions  $\chi_i$ . Following Ref. [43], the Hamiltonian of this model is [48, 49]

$$H = \sum_{i < j < k < l} J_{ijkl} \chi_i \chi_j \chi_k \chi_l \quad (13)$$

and the  $M = mN$  jump operators are given by

$$W_m = i \sum_{i < j} \ell_{m,ij} \chi_i \chi_j. \quad (14)$$

The couplings  $J_{ijkl}$  and  $\ell_{m,ij}$  are independent Gaussian random variables with zero mean and variance

$$\langle J_{ijkl}^2 \rangle = \frac{3!J^2}{N^3} \quad \text{and} \quad \langle |\ell_{m,ij}|^2 \rangle = \frac{\gamma^2}{N^2}, \quad (15)$$

respectively. The coefficients  $J_{ijkl}$  must be real to ensure the Hermiticity of the Hamiltonian, while  $\ell_{m,ij}$  are taken to be complex. We set  $J = m = \gamma = 1$ .

Finally, we employ the damped tilted-field Ising model of Ref. [26], which has local interactions and dissipation but spatial disorder. The Hamiltonian is given by

$$H = \sum_{i=1}^{L-1} \sigma_i^z \sigma_{i+1}^z + g \sum_{i=1}^L \sigma_i^x + \sum_{i=1}^L h_i \sigma_i^z, \quad (16)$$

where  $\sigma_i^\alpha$  ( $\alpha = x, y, z$ ) are the standard Pauli matrices on site  $i$ ,  $g = 0.9$  is a constant transverse field, and the disordered longitudinal field  $h_i$  is taken randomly from  $[-h, +h]$  with  $h = 0.2$ ; the jump operators are  $W_k = \sqrt{\mu/2} \sigma_k^z$ , with  $k = 1, 2, \dots, L$  and  $\mu = 0.4$ . We use open boundary conditions.

*Universality of Lindbladian ETH.*—We now show the universality of Lindbladian ETH by computing the local scalings and distributions of OR,  $L\rho$ , and LL in the three models introduced above. For the random Liouvillian, the observable is  $O = O_2 \otimes 1_{\mathcal{D}/2}$ , where  $O_2$  is a  $2 \times 2$  random matrix from the Gaussian orthogonal

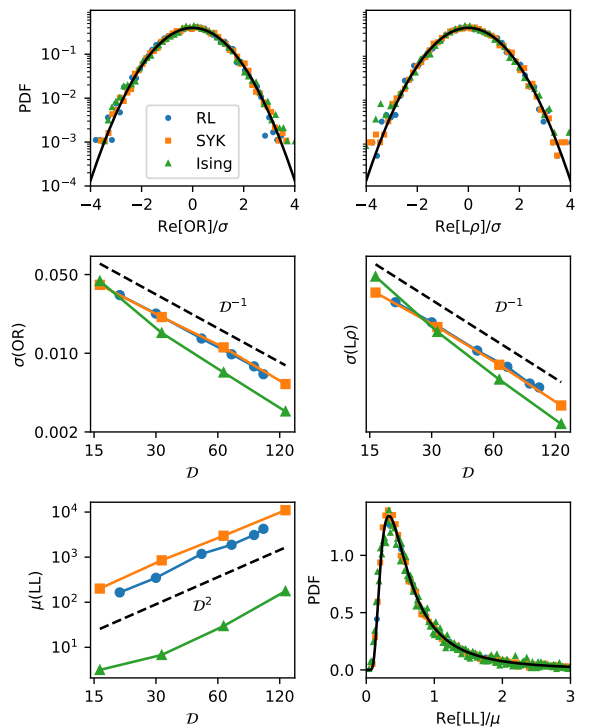


Figure 2. Verification of the Lindbladian ETH ansatz for random Liouvillians, the dissipative SYK model (with observable  $O = \chi_1 \chi_2 \chi_3 \chi_4$ ), and a damped Ising chain. (Top row) Distribution of OR (left) and  $L\rho$  (right), normalized by the respective standard deviations. The colored dots are histograms for the three different models, which are compared with a standard Gaussian distribution (black line). (Middle row) Scaling of the width of the distribution with the Hilbert space dimension  $\mathcal{D}$ . In all three models, OR (left) and  $L\rho$  (right) scale as  $\mathcal{D}^{-1}$  (dashed line). (Bottom row, left) Scaling of the mean of LL, compared with the RMT prediction,  $\mathcal{D}^2$  (dashed line). (Bottom row, right) Distribution of LL normalized by its mean. The black line is the  $1/\gamma_2$  distribution, which is followed in all three physical models.

ensemble and the initial state is  $\rho = |0\rangle\langle 0|$  for an arbitrary computational basis state  $|0\rangle$  in the many-body Hilbert space. In the SYK model, we consider two different observables,  $O = i\chi_1 \chi_2$  and  $O = \chi_1 \chi_2 \chi_3 \chi_4$ , and the initial state is  $\rho = |\Omega\rangle\langle \Omega|$  where  $|\Omega\rangle$  is the fermionic vacuum of a single copy of the SYK model. In the Ising model, the observable is  $O = \sigma_{L/2}^x$  and the initial state is  $\rho = |\uparrow \dots \uparrow\rangle\langle \uparrow \dots \uparrow|$ , where  $|\uparrow \dots \uparrow\rangle$  is the  $L$ -fold tensor product of the  $+1$  eigenstate of  $\sigma^z$ . We select a small region in the bulk of the complex spectrum (see Fig. 1), compute the three quantities for approximately  $10^5/\mathcal{D}^2$  independent realizations, and determine their average, variance, and full distribution. The results are shown in Fig. 2 and confirm the validity of the Lindbladian ETH ansatz: in all three models, OR and  $L\rho$  have a complex Gaussian distribution and scale as  $\mathcal{D}^{-1}$ , while LL has a  $1/\gamma_2$  distribution and scales as  $\mathcal{D}^2$ .

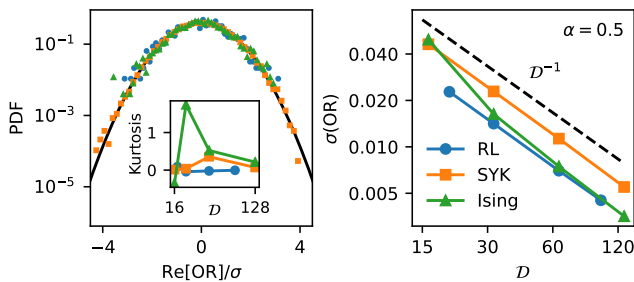


Figure 3. Distribution (left) and scaling of the variance with Hilbert space dimension (right) of  $\text{Re}[OR]$  for  $\alpha = 0.5$  in the three physical models. Here, we use  $\mu = 0.8$  for the Ising model to converge faster to the RMT regime. Despite the loss of trace preservation, the scaling of the variances is still that predicted by the Lindblad ETH ansatz for all models. Moreover, the full distribution follows a Gaussian, while there are deviations in the tails for the Ising model. In the inset of the left panel, we compute the excess kurtosis, which is zero for a Gaussian distribution, as a function of the Hilbert space dimension; for all models, it decreases with system size.

*Robustness of Lindbladian ETH.*—We now show that Lindbladian ETH is robust and is still valid when trace preservation is relaxed. To this end, we introduce a deformed Liouvillian given by

$$\mathcal{L}_\alpha[\rho] = -iK\rho + i\rho K^\dagger + \alpha \sum_k W_k \rho W_k^\dagger, \quad (17)$$

where  $K = H - \frac{i}{2} \sum_k W_k^\dagger W_k$  is an effective non-Hermitian Hamiltonian. Here,  $\alpha \in [0, 1]$  quantifies the trace preservation (i.e., probability conservation) of the dynamics, with  $\mathcal{L}_{\alpha=1}$  the usual Lindbladian. The regime  $\alpha < 1$  corresponds to postselecting only trajectories with a fraction  $\alpha$  of jumps (“dilute-click regime”), as shown in the End Matter. The dynamics under  $\mathcal{L}_{\alpha=0}$  arises in the no-click limit [50–52], where only quantum trajectories without quantum jumps are postselected. In this limit,  $\mathcal{L}_0$  reduces to two decoupled replicas of a non-Hermitian Hamiltonian.

The distribution and scaling of OR for  $\alpha = 0.5$  are shown in Fig. 3. For random Liouvillians and the SYK model, OR is still Gaussian distributed and scales with  $\mathcal{D}^{-1}$ , as predicted by our Lindbladian ETH ansatz. For the damped Ising model, the scaling matches the prediction but there are deviations in the tails of the distribution. To investigate this discrepancy, we compute the excess kurtosis of the distribution, which is zero for a Gaussian, as a function of  $\mathcal{D}$  for all three models, see the inset of Fig. 3. For the random Liouvillian, it is consistent with zero for all system sizes, while for the SYK model it decreases to close to zero at  $\mathcal{D} \sim 100$ . For the Ising model, the available system sizes do not allow us to reach a definitive conclusion, but the data is consistent with an approach to Gaussianity in the thermodynamic limit, albeit at a much slower rate than for the other two

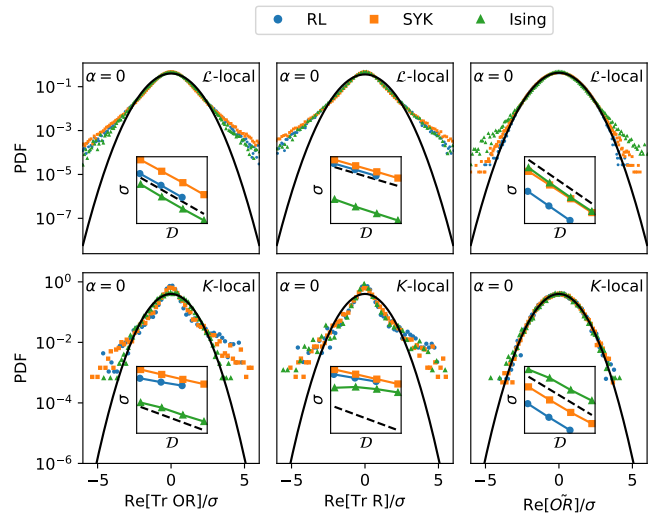


Figure 4. Distribution of  $\text{Tr}[OR]$ ,  $\text{Tr} R$ , and  $\widetilde{OR} \equiv \text{Tr}[OR] - \overline{O} \text{Tr} R$  for  $\alpha = 0$  in random Liouvillians, the dissipative SYK model and the damped Ising chain. In the top row, the distributions are computed in a small region of the spectrum of  $\mathcal{L}_0$ , while in the bottom row they are computed locally in the spectrum of  $K$ . (Insets) The scaling of the variance of the distributions with the Hilbert space dimension is compared with  $\mathcal{D}^{-1/2}$  (black dashed line). Here, the eigenvalue window is chosen as  $[\mu_x - \sigma_x/5, \mu_x + \sigma_x/5] \times [\sigma_y/5, 2\sigma_y/5]$  and for the SYK model we take  $O = i\chi_1\chi_2$  as the observable.

models (which are more disordered and less constrained by locality).

A similar agreement is found for  $L\rho$  and LL and for other values of  $\alpha > 0$ . More generally, we expect Lindbladian ETH to hold as long as the dynamical generator couples the two copies of the Hilbert space (i.e., the bra and the ket of the density matrix), as a generic Hermiticity-preserving generator does.

*Limits of Lindbladian ETH.*—The condition mentioned in the previous paragraph fails for  $\alpha = 0$ , where the jump contribution vanishes, the two copies decouple, and the Liouvillian corresponds to a doubled non-Hermitian Hamiltonian. The right eigenoperators of  $\mathcal{L}_0$  are given by  $R_{mn} = |r_m\rangle\langle r_n|$  and have eigenvalues  $\lambda_{nm} = -i(\varepsilon_n - \varepsilon_m^*)$ , where  $|r_n\rangle$  is the right eigenvector of  $K$  with eigenvalue  $\varepsilon_n$ ,  $K|r_n\rangle = \varepsilon_n|r_n\rangle$ . Due to this additional structure, and using Eq. (2) [28], the right-eigenvector overlap  $\text{Tr}[OR_{mn}]$  becomes

$$\text{Tr}[OR_{mn}] = \overline{O} \text{Tr}[R_{mn}] + S_{mn} \sqrt{\frac{O^2}{\mathcal{D}}}. \quad (18)$$

Although the random variable  $S_{mn}$  follows a normal distribution when  $\varepsilon_n \approx \varepsilon_m$  (i.e., locally within the spectrum of  $K$ ), it may deviate from a Gaussian when  $\varepsilon_n$  and  $\varepsilon_m$  are far apart, which is generically the case in a small window around  $\lambda_{nm}$  (i.e., locally within the spectrum of  $\mathcal{L}_0$ ). Figure 4 confirms this behavior in the three physi-

cal models. Furthermore, the quantity  $\text{Tr}[R_{mn}]$  exhibits a non-Gaussian distribution with heavy tails across all three models, as also shown in Fig. 4. Consequently, the OR overlap becomes generically non-Gaussian and the Lindbladian ETH ansatz breaks down at  $\alpha = 0$  (in the End Matter we provide further evidence that the ansatz breaks down only in the no-click limit). Note, however, that even though the distribution is non-Gaussian, its variance still has the predicted scaling  $\mathcal{D}^{-1/2}$ .

To confirm that non-Hermitian ETH [28], Eq. (2), instead holds locally in the spectrum of  $K$ , we computed the same quantities for that case; they are depicted in the bottom row of Fig. 4. While  $\text{Tr}[OR]$  and  $\overline{O} \text{Tr} R$  remain non-Gaussian, their difference  $\overline{OR} \equiv \text{Tr}[OR] - \overline{O} \text{Tr} R$  (which is proportional to  $S_{nm}$ ) follows a Gaussian distribution and scales as  $\mathcal{D}^{-1/2}$ . In contrast, even  $\overline{OR}$  is non-Gaussian locally in the spectrum of  $\mathcal{L}_0$ .

*Conclusions.*—In this work, we studied the quantities that govern the dissipative dynamics of generic observables across several physical models. Our results show that these quantities exhibit universal scalings and distributions, similarly to ETH in isolated systems. By introducing a deformation parameter  $\alpha \in [0, 1]$ , we found that the ansatz is robust against the loss of trace preservation ( $0 < \alpha < 1$ ). However,  $\alpha = 0$  is a strikingly different case, as the Lindbladian decouples into two non-Hermitian Hamiltonians and Lindbladian ETH is destroyed.

This work paves the way for a deeper understanding of the structure of Lindblad eigenvectors in open quantum systems, paralleling the success of ETH in the context of closed systems. Contrary to the case of isolated systems, in which ETH helps explain the relaxation of observables to a local thermal equilibrium, the fate of open quantum systems is always the steady state, which need not even be thermal. As such, the implications of the ETH structure of the overlaps studied in this work remain an interesting open question with significant impact in the understanding of the dynamical behaviour of generic open quantum systems.

*Acknowledgments.*—GA and PR acknowledge support by FCT through Grant No. UID/CTM/04540 to the I&D unit Centro de Física e Engenharia de Materiais Avançados. This work was produced with the support of INCD funded by FCT and FEDER under the project 01/SAICT/2016 n<sup>o</sup> 022153. This work was realized within the QuantERA ERA-NET project DQUANT: A Dissipative Quantum Chaos perspective on Near-Term Quantum Computing, supported by FCT-Portugal Grant Agreement No. 101017733.<sup>1</sup> MH acknowledges support from the Deutsche Forschungsgemeinschaft under grant SFB 1143 (project-id 247310070). LS was supported by a Research Fellowship from the Royal Com-

mission for the Exhibition of 1851.

\* gabriel.m.almeida@tecnico.ulisboa.pt

† ribeiro.pedro@tecnico.ulisboa.pt

‡ ld710@cam.ac.uk

- [1] J. M. Deutsch, Quantum statistical mechanics in a closed system, *Phys. Rev. A* **43**, 2046 (1991).
- [2] M. Srednicki, Chaos and quantum thermalization, *Phys. Rev. E* **50**, 888 (1994).
- [3] M. Rigol, V. Dunjko, and M. Olshanii, Thermalization and its mechanism for generic isolated quantum systems, *Nature* **452**, 854 (2008).
- [4] M. Rigol and L. F. Santos, Quantum chaos and thermalization in gapped systems, *Phys. Rev. A* **82**, 011604 (2010).
- [5] A. Polkovnikov, K. Sengupta, A. Silva, and M. Vengalattore, Colloquium: Nonequilibrium dynamics of closed interacting quantum systems, *Rev. Mod. Phys.* **83**, 863 (2011).
- [6] L. F. Santos and M. Rigol, Localization and the effects of symmetries in the thermalization properties of one-dimensional quantum systems, *Phys. Rev. E* **82**, 031130 (2010).
- [7] W. Beugeling, R. Moessner, and M. Haque, Finite-size scaling of eigenstate thermalization, *Phys. Rev. E* **89**, 042112 (2014).
- [8] R. Nandkishore and D. A. Huse, Many-Body Localization and Thermalization in Quantum Statistical Mechanics, *Ann. Rev. Cond. Matt. Phys.* **6**, 15 (2015).
- [9] L. D'Alessio, Y. Kafri, A. Polkovnikov, and M. Rigol, From quantum chaos and eigenstate thermalization to statistical mechanics and thermodynamics, *Adv. Phys.* **65**, 239 (2016).
- [10] R. Mondaini and M. Rigol, Eigenstate thermalization in the two-dimensional transverse field Ising model. II. Off-diagonal matrix elements of observables, *Phys. Rev. E* **96**, 012157 (2017).
- [11] S. Ziraldo and G. E. Santoro, Relaxation and thermalization after a quantum quench: Why localization is important, *Phys. Rev. B* **87**, 064201 (2013).
- [12] T. N. Ikeda, Y. Watanabe, and M. Ueda, Finite-size scaling analysis of the eigenstate thermalization hypothesis in a one-dimensional interacting Bose gas, *Phys. Rev. E* **87**, 012125 (2013).
- [13] V. Alba, Eigenstate thermalization hypothesis and integrability in quantum spin chains, *Phys. Rev. B* **91**, 155123 (2015).
- [14] X. Li, S. Ganeshan, J. H. Pixley, and S. Das Sarma, Many-Body Localization and Quantum Nonergodicity in a Model with a Single-Particle Mobility Edge, *Phys. Rev. Lett.* **115**, 186601 (2015).
- [15] S. Nandy, A. Sen, A. Das, and A. Dhar, Eigenstate Gibbs ensemble in integrable quantum systems, *Phys. Rev. B* **94**, 245131 (2016).
- [16] J. M. Magán, Random Free Fermions: An Analytical Example of Eigenstate Thermalization, *Phys. Rev. Lett.* **116**, 030401 (2016).
- [17] M. Haque and P. A. McClarty, Eigenstate thermalization scaling in Majorana clusters: From chaotic to integrable Sachdev-Ye-Kitaev models, *Phys. Rev. B* **100**, 115122 (2019).

<sup>1</sup> <https://doi.org/10.54499/QuantERA/0003/2021>

- (2019).
- [18] M. Mierzejewski and L. Vidmar, Quantitative Impact of Integrals of Motion on the Eigenstate Thermalization Hypothesis, *Phys. Rev. Lett.* **124**, 040603 (2020).
- [19] J. D. Noh, Eigenstate thermalization hypothesis and eigenstate-to-eigenstate fluctuations, *Phys. Rev. E* **103**, 012129 (2021).
- [20] H. Bernien, S. Schwartz, A. Keesling, H. Levine, A. Omran, H. Pichler, S. Choi, A. S. Zibrov, M. Endres, M. Greiner, *et al.*, Probing many-body dynamics on a 51-atom quantum simulator, *Nature* **551**, 579 (2017).
- [21] C. J. Turner, A. A. Michailidis, D. A. Abanin, M. Serbyn, and Z. Papić, Weak ergodicity breaking from quantum many-body scars, *Nat. Phys.* **14**, 745 (2018).
- [22] N. Shiraishi and T. Mori, Systematic Construction of Counterexamples to the Eigenstate Thermalization Hypothesis, *Phys. Rev. Lett.* **119**, 030601 (2017).
- [23] M. Serbyn, D. A. Abanin, and Z. Papić, Quantum many-body scars and weak breaking of ergodicity, *Nat. Phys.* **17**, 675–685 (2021).
- [24] S. Moudgalya, B. A. Bernevig, and N. Regnault, Quantum many-body scars and Hilbert space fragmentation: a review of exact results, *Rep. Prog. Phys.* **85**, 086501 (2022).
- [25] S. Moudgalya, T. Devakul, D. P. Arovas, and S. L. Sondhi, Extension of the eigenstate thermalization hypothesis to nonequilibrium steady states, *Phys. Rev. B* **100**, 045112 (2019).
- [26] R. Hamazaki, M. Nakagawa, T. Haga, and M. Ueda, Lindbladian many-body localization, [arXiv:2206.02984](https://arxiv.org/abs/2206.02984) (2022).
- [27] G. Cipolloni and J. Kudler-Flam, Non-Hermitian Hamiltonians violate the eigenstate thermalization hypothesis, *Phys. Rev. B* **109**, L020201 (2024).
- [28] S. S. Roy, S. Bandyopadhyay, R. C. de Almeida, and P. Hauke, Unveiling Eigenstate Thermalization for Non-Hermitian Systems, [arXiv:2309.00049](https://arxiv.org/abs/2309.00049) (2023).
- [29] J. Richter, L. Sá, and M. Haque, Integrability versus chaos in the steady state of many-body open quantum systems, [arXiv:2412.16041](https://arxiv.org/abs/2412.16041) (2024).
- [30] A. M. García-García, Z. Lu, L. Sá, and J. J. M. Verbaarschot, Lindblad many-body scars, [arXiv:2503.06665](https://arxiv.org/abs/2503.06665) (2025).
- [31] Y. Ashida, Z. Gong, and M. Ueda, Non-Hermitian physics, *Adv. Phys.* **69**, 249 (2020).
- [32] H.-P. Breuer and F. Petruccione, *The Theory of Open Quantum Systems* (Oxford University Press, Oxford, 2002).
- [33] G. Lindblad, On the generators of quantum dynamical semigroups, *Commun. Math. Phys.* **48**, 119 (1976).
- [34] V. Gorini, A. Kossakowski, and E. C. G. Sudarshan, Completely positive dynamical semigroups of N-level systems, *J. Math. Phys.* **17**, 821 (1976).
- [35] J. T. Chalker and B. Mehlige, Eigenvector Statistics in Non-Hermitian Random Matrix Ensembles, *Phys. Rev. Lett.* **81**, 3367 (1998).
- [36] B. Mehlige and J. T. Chalker, Statistical properties of eigenvectors in non-Hermitian Gaussian random matrix ensembles, *J. Math. Phys.* **41**, 3233 (2000).
- [37] P. Bourgade and G. Dubach, The distribution of overlaps between eigenvectors of Ginibre matrices, *Prob. Theory Relat. Fields* **177**, 397 (2020).
- [38] S. Denisov, T. Laptjeva, W. Tarnowski, D. Chruściński, and K. Życzkowski, Universal Spectra of Random Lindblad Operators, *Phys. Rev. Lett.* **123**, 140403 (2019).
- [39] T. Can, Random Lindblad dynamics, *J. Phys. A* **52**, 485302 (2019).
- [40] T. Can, V. Oganesyan, D. Orgad, and S. Gopalakrishnan, Spectral Gaps and Midgap States in Random Quantum Master Equations, *Phys. Rev. Lett.* **123**, 234103 (2019).
- [41] L. Sá, P. Ribeiro, and T. Prosen, Spectral and steady-state properties of random Liouvillians, *J. Phys. A* **53**, 305303 (2020).
- [42] W. Tarnowski, I. Yusipov, T. Laptjeva, S. Denisov, D. Chruściński, and K. Życzkowski, Random generators of Markovian evolution: A quantum-classical transition by superdecoherence, *Phys. Rev. E* **104**, 034118 (2021).
- [43] L. Sá, P. Ribeiro, and T. Prosen, Lindbladian dissipation of strongly-correlated quantum matter, *Phys. Rev. Res.* **4**, L022068 (2022).
- [44] A. Kulkarni, T. Numasawa, and S. Ryu, Lindbladian dynamics of the Sachdev-Ye-Kitaev model, *Phys. Rev. B* **106**, 075138 (2022).
- [45] A. M. García-García, L. Sá, J. J. M. Verbaarschot, and J. P. Zheng, Keldysh wormholes and anomalous relaxation in the dissipative Sachdev-Ye-Kitaev model, *Phys. Rev. D* **107**, 106006 (2023).
- [46] K. Kawabata, A. Kulkarni, J. Li, T. Numasawa, and S. Ryu, Dynamical quantum phase transitions in Sachdev-Ye-Kitaev Lindbladians, *Phys. Rev. B* **108**, 075110 (2023).
- [47] A. M. García-García, L. Sá, J. J. M. Verbaarschot, and C. Yin, Emergent topology in many-body dissipative quantum matter, *Phys. Rev. B* **111**, 035157 (2025).
- [48] A. Kitaev, A simple model of quantum holography (2015), string seminar at KITP and Entanglement 2015 program, 12 February, 7 April, and 27 May 2015, <http://online.kitp.ucsb.edu/online/entangled15/>.
- [49] J. Maldacena and D. Stanford, Remarks on the Sachdev-Ye-Kitaev model, *Phys. Rev. D* **94**, 106002 (2016).
- [50] J. Dalibard, Y. Castin, and K. Mølmer, Wave-function approach to dissipative processes in quantum optics, *Phys. Rev. Lett.* **68**, 580 (1992).
- [51] P. Zoller, M. Marte, and D. F. Walls, Quantum jumps in atomic systems, *Phys. Rev. A* **35**, 198 (1987).
- [52] P. M. Visser and G. Nienhuis, Solution of quantum master equations in terms of a non-Hermitian Hamiltonian, *Phys. Rev. A* **52**, 4727 (1995).

END MATTER

### Dilute-click regime

In this Appendix, we show that the deformed Liouvillian in Eq. (17) effectively reduces the jump rate by a factor of  $\alpha$ , meaning that quantum trajectories with jumps are accepted only with probability  $\alpha$ . This post-selection interpretation can be seen as follows.

For a small time step  $\delta t$ , the density matrix evolves as

$$\begin{aligned} \rho(t + \delta t) \approx & (1 - iK\delta t)\rho(t)(1 + iK^\dagger\delta t) \\ & + \alpha\delta t \sum_k W_k\rho(t)W_k^\dagger. \end{aligned} \quad (19)$$

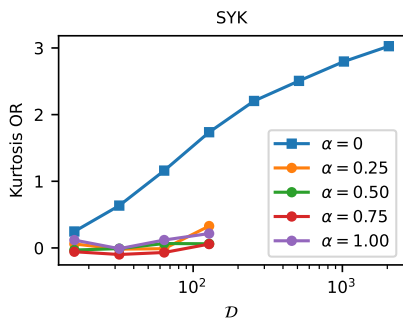


Figure 5. Excess kurtosis of the distribution of OR as function of the Hilbert space dimension in the dissipative SYK model (with observable  $O = i\chi_1\chi_2$ ) for different values of  $\alpha$ . A value of zero corresponds to a Gaussian distribution, which is attained for all  $\alpha > 0$ ; for  $\alpha = 0$ , the kurtosis increases rapidly with  $\mathcal{D}$ , which signals a strong deviation from Gaussianity and a breakdown of Lindbladian ETH.

The first term corresponds to evolution without jumps, while the second term accounts for the possibility of jumps occurring. To interpret this evolution probabilistically, we define the normalized (unit-trace) density matrices

$$\rho^{(0)} = \frac{(1 - iK\delta t)\rho(t)(1 + iK^\dagger\delta t)}{p_0}, \quad (20)$$

$$\rho^{(k)} = \frac{\alpha\delta t W_k \rho(t) W_k^\dagger}{\delta p_k}, \quad (21)$$

with the associated probabilities

$$p_0 = \text{Tr}[(1 - iK\delta t)\rho(t)(1 + iK^\dagger\delta t)], \quad (22)$$

$$\delta p_k = \alpha\delta t \text{Tr}[W_k \rho(t) W_k^\dagger]. \quad (23)$$

Thus, the evolved density matrix takes the form

$$\rho(t + \delta t) = p_0 \rho^{(0)} + \sum_k \delta p_k \rho^{(k)}. \quad (24)$$

This is a statistical mixture of  $\rho^{(0)}$ , which corresponds to the evolution if no jump occurs, and states  $\rho^{(k)}$ , which are the collapsed states following a jump associated with  $W_k$ . Unless  $\alpha = 1$ , we have  $p_0 + \sum_k p_k < 1$ , meaning that the evolved density matrix has trace less than 1. The missing trace corresponds to the probability of trajectories with jumps that were discarded in the post-selection process.

Note that, as in the no-click limit, the Liouvillian studied in the main text differs from the generator of the diluted click dynamics given above by a constant factor that is a non-linear function of the density matrix. Therefore, although the evolution with the linear Liouvillian reproduces the correct density matrix, it is not able to capture the probability of the dilute click trajectories, similarly to the no-click limit.

Since  $\delta p_k = \alpha \delta p_k|_{\alpha=1}$ , this evolution corresponds to, at each time step, accepting a jump only with probability  $\alpha$ . In the no-click limit,  $\alpha = 0$ , jumps are completely discarded and the system evolves under the non-Hermitian Hamiltonian  $K$ . For  $\alpha = 1$ , we recover the standard trace-preserving Lindblad evolution, where jumps occur with their original probability. For intermediate values  $0 < \alpha < 1$ , the system follows a “diluted jump” regime, where jumps occur less frequently than in the standard Lindblad evolution.

#### No-click limit

In this Appendix, we further substantiate the claim that the distributions become non-Gaussian only at the singular point  $\alpha = 0$  (no-click limit), while Lindbladian ETH holds for any nonzero  $\alpha$ . In Fig. 5, we plot the excess kurtosis as a function of the Hilbert space dimension for the dissipative SYK model with different  $\alpha$ . It remains close to zero for  $\alpha = 0.25, \dots, 1$ , while it grows steeply with  $\mathcal{D}$  at the singular point  $\alpha = 0$ .